JOURNAL OF GUIDANCE, CONTROL, AND DYNAMICS
Vol. 21, No. 1, January–February 1998

Rapid Hover-to-Forward-Flight Transitions for a Thrust-Vectored Aircraft

Michiel J. Van Nieuwstadt* and Richard M. Murray†
California Institute of Technology, Pasadena, California 91125

The use of differential flatness for computation of a nominal trajectory for fast transition between flight modes of autonomous vehicles is investigated. Differential flatness of an approximate model of the longitudinal dynamics of a thrust-vectored aircraft is used to achieve fast switching between flight modes. We conclude that steering to the trimmed state of the full model is of crucial importance for good performance. Simulations and experimental data for a thrust-vectored flight-control experiment at Caltech are provided to validate the approach.

Nomenclature

C_x = horizontal aerodynamic coefficient
C_y = vertical aerodynamic coefficient
C_θ = rotational aerodynamic coefficient
$\bar{c}$ = mean aerodynamic chord, m
D = aerodynamic drag, N
J = inertia, kg · m^2
L = aerodynamic lift, N
M = aerodynamic moment, Nm
m_g = gravitational mass, kg
m_x = inertial mass in x direction, kg
m_z = inertial mass in z direction, kg
Q = pitch rate, rad/s
r = distance from center of mass to point where thrust acts, m
S = wing surface, m^2
T_1 = forward thrust, N
T_2 = downward thrust, N
U = forward body velocity, m/s
V = absolute velocity, m/s
W = downward body velocity, m/s
x = spatial horizontal coordinate, m/s, *or* state of a system
x_f = x coordinate of the center of oscillation
z = spatial vertical coordinate, m/s, *or* flat output
z_f = z coordinate of the center of oscillation
α = angle of attack, rad
δ = elevator, deg
Θ = angle of aircraft with the vertical: $\theta - \pi/2$, rad
θ = pitch angle, rad
ρ = density, kg/m^3

I. Introduction

THE use of modern control in commercial aircraft is typically restricted to stability augmentation and setpoint tracking. Commercial aircraft have been flying successfully with simple linear controllers based on frequency-domain analysis for many years,[1,2] and there seems to be little need for advanced control methodologies for commercial aircraft. On the other hand, substantial research effort in flight control has been focused on increasingly autonomous flight. Among the application areas of autonomous flight are highly maneuverable military aircraft and remotely piloted vehicles for reconnaissance missions. It is to such aircraft that the techniques presented in this paper can be applied.

Highly maneuverable aircraft offer both the potential and the need for more advanced control methodologies to fully exploit their maneuvering potential.[3–5] The dynamics and actuator effectiveness of an aircraft, as well as the controlled variables, may change dramatically over different parts of a maneuver and from one maneuver to the next. Use of the knowledge of the nonlinear dynamics in the control system is essential for this type of aircraft.

Remotely piloted vehicles receive only low-frequency feedback from a human pilot. The onboard control system must have sufficient autonomy to determine the flight path and corresponding actuators, either from goal points provided by a human pilot, or the location of a moving target provided by onboard sensors. It is clear that inclusion of knowledge of the nonlinear dynamics of the vehicle in the control system will greatly improve its performance.

We advocate an approach to combine nonlinear control theory with linear techniques, which consists of generating a feasible full state trajectory for the nominal nonlinear system and using linear theory to stabilize the local linear approximation. Use of nonlinear feedforward provides better performance than when relying entirely on linear techniques. This requires efficient computational techniques that allow online computation of the nonlinear portion of the controller.

We concentrate on the pitch dynamics of a thrust-vectored aircraft. The benefit of thrust vectoring is mostly in the pitch dynamics, because it allows flight at high angle of attack. It is well known that under fairly mild assumptions (rigid body, longitudinal plane of symmetry), the pitch dynamics decouple from the lateral dynamics. A study of pitch dynamics alone therefore is justified. We first derive the rigid-body pitch dynamics of the aircraft, resulting from the thrust vectoring. If we ignore the aerodynamic forces, the thrust-vectoring dynamics have a special property, namely, differential flatness, that makes trajectory generation trivial. We use differential flatness of the thrust-vectoring model to compute nominal trajectories for the aircraft. These trajectories are only approximately feasible, because they do not take into account the aerodynamic forces. We are therefore dealing with an approximately flat system with perturbations. The focus of this paper is the investigation of several extensions to compensate for the discrepancy between the flat approximate model and the full aerodynamic model. The particular application that we use to demonstrate our techniques is the transition from hover to forward flight for the thrust-vectored aircraft, which we call mode switching. This is just one out of a multitude of transitions between different flight modes, and one that is particularly appropriate for a thrust-vectored aircraft. It should be pointed out that the property of differential flatness is highly nongeneric, and hence the techniques presented in this paper do not extend to general aircraft. A fairly broad class of aircraft models has been shown to be differentially flat.[6]

The organization of the paper is as follows. The two-degree-of-freedom (DOF) control methodology and the concept of differential flatness are explained in Sec. II. In Sec. III, we present the general pitch dynamics of an aircraft, first from thrust vectoring only, then with aerodynamic forces included. We also present the various aerodynamic functions identified from wind-tunnel data on a model thrust-vectored aircraft built at the California Institute of Technology (Caltech). In Sec. IV, we discuss how we can deal with

Received Sept. 12, 1996; revision received June 30, 1997; accepted for publication July 1, 1997.

*Graduate Student, Division of Engineering and Applied Science.

†Professor, Division of Engineering and Applied Science.

the perturbations to the flat model using Lyapunov arguments and present simulations to illustrate the approach. Experimental data are provided in Sec. V to validate the approach. An abbreviated version of this paper has appeared elsewhere.[7]

II. Control Methodology

A. Differential Flatness

Differential flatness was originally introduced by Fliess et al.[8] in a differentially algebraic context and later using Lie–Bäcklund transformations.[9] The important property of flat systems is that we can find a set of outputs (equal in number to the number of inputs) such that we can express all states and inputs in terms of those outputs and their derivatives. More precisely, a nonlinear system

$$\begin{aligned} \dot{x} &= f(x,u) \qquad x \in \boldsymbol{R}^n,\ u \in \boldsymbol{R}^m \\ y &= h(x) \qquad y \in \boldsymbol{R}^m \end{aligned} \tag{1}$$

is differentially flat if we can find outputs $z \in \boldsymbol{R}^m$ of the form

$$z = \zeta\left(x, u, \dot{u}, \ldots, u^{(l)}\right) \tag{2}$$

such that

$$\begin{aligned} x &= x\left(z, \dot{z}, \ldots, z^{(l)}\right) =: x(\bar{z}) \\ u &= u\left(z, \dot{z}, \ldots, z^{(l)}\right) =: u(\bar{z}) \end{aligned} \tag{3}$$

We call y the tracking outputs and z the flat outputs. These outputs are not necessarily the same and care must be taken when the tracking outputs result in right half-plane zeros for the linearized system, in order to avoid exciting instabilities in the internal dynamics. For ease of notation, we stack the flat outputs and their derivatives in the flat flag, $\bar{z} := (z, \dot{z}, \ldots, z^{(l)})$.

Differentially flat systems are useful in situations in which explicit trajectory generation is required. Because the behavior of flat systems is determined by the flat outputs, we can plan trajectories in output space, and then map these to appropriate inputs. A common example is a kinematic car, in which the xy position of the rear wheels provides flat outputs. This implies that all feasible trajectories of the system can be determined by specifying only the trajectory of the rear wheels. This idea is illustrated in more detail in the following sections.

Differential flatness also can be characterized using tools from exterior differential systems.[10] In the beginning of this century, the French mathematician E. Cartan developed this set of powerful tools for the study of equivalence of systems of differential equations.[11–13] Equivalence need not be restricted to systems of equal dimensions. In particular, a system can be prolonged to a bigger system on a bigger manifold, and equivalence between these prolongations can be studied. Two systems that have equivalent prolongations are called absolutely equivalent. Differentially flat systems can be interpreted as being those systems that are absolutely equivalent to the trivial system, i.e., having no dynamic constraints on the free variables.[10]

B. Two-DOF Design

Linear control of aircraft is a well-established discipline with a vast knowledge base. One would like to combine this knowledge from traditional linear theory with the advanced concepts of nonlinear control theory to arrive at an optimal synthesis. Two-DOF design offers such a synthesis. It is a control paradigm, depicted in Fig. 1, consisting of two blocks: a trajectory generation block and a feedback compensation block.

The purpose of the trajectory generation block is to synthesize a feasible state-space trajectory for the system, given a desired reference signal. For example, the reference signal might be the desired position of the center of mass of an aircraft. This trajectory may or may not be something that can actually be executed by the aircraft, either because of limitations on the actuation system or because there does not exist a trajectory in state space that simultaneously satisfies the equations of motion and gives the desired trajectory for the center of mass. It is the responsibility of the trajectory generation block to use this reference signal to generate a feasible state-space trajectory, as well as a set of nominal inputs that drive the system along this path.

Given the feasible state-space trajectory, the feedback compensation block is used to correct for any errors due to noise or plant uncertainty (depicted in Fig. 1 as a feedback with unknown parameters Δ). Given the desired state-space trajectory x_d, the error dynamics then can be written as a time-varying control system in terms of the state error $e = x - x_d$. Under the assumption that the tracking error remains small, we can linearize this time-varying system about $e = 0$ and stabilize the $e = 0$ state.

We show through simulation and experiment that the use of a nominal trajectory gives a more aggressive response than point stabilization around a changing output, while reducing control effort. This shows that for aggressive maneuvering we should exploit the nonlinearities of the aircraft to obtain better performance.

The two-DOF approach encompasses several well-known paradigms. Optimal control[14] is among the older ones. Optimal-control theory provides an extremely elegant solution to many trajectory generation problems. However, optimal control leads to a two-point boundary value problem and the computational requirements are heavy, especially for higher-dimensional examples. We

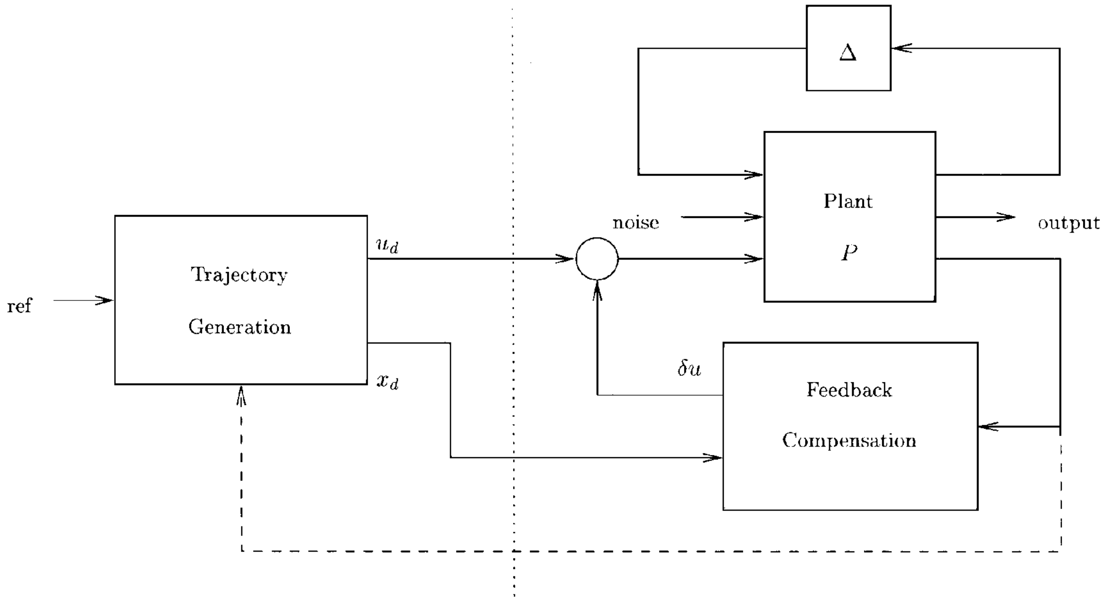

Fig. 1 Two-DOF controller design.

concentrate on suboptimal trajectory generation methods that are computationally much more efficient, for which numerical convergence is guaranteed, and that can be performed onboard the vehicle in real time.

Autopilots use a very simple type of trajectory generation, namely, an interpolation between initial and final state without regard for the system dynamics. The resulting trajectory is not, in general, feasible.

Dynamic inversion[15] is a popular approach in aircraft control, that is not, strictly speaking, a two-DOF design. It refers to the practice of inverting part of the system dynamics, so that accelerations are commanded instead of forces. Unless the system is fully actuated, the resulting system is not linear. Dynamic inversion does not generate a feasible full state-space trajectory.

III. Pitch Dynamics

We first present the rigid-body pitch dynamics of an aircraft resulting from the thrust vectoring. Then we add aerodynamic forces. The reason for this two-stage development is that the rigid-body dynamics are flat, whereas the aerodynamic forces act as perturbation terms. Note that a conventional aircraft with one thrust DOF, and aerodynamic surfaces, is flat, under some reasonable assumptions.[6] Thus, the techniques described here also might be applied to more general control problems.

A. Thrust-Vectoring Dynamics

Consider the thrust-vectored aircraft with wing depicted in Figs. 2 and 3. Note here that (x, z) are inertial coordinates and (U, W) are body velocities.

For hover-to-hover transitions, we want to control the position of the aircraft with respect to a fixed spatial frame. Hover-to-hover transitions typically happen at low speed. We therefore ignore the aerodynamic effects of drag and lift. The pitch dynamics in spatial coordinates are then

$$\begin{pmatrix} m_x\ddot{x} \\ m_z\ddot{z} \\ J\ddot{\theta} \end{pmatrix} = \begin{pmatrix} \cos\theta & \sin\theta \\ -\sin\theta & \cos\theta \\ 0 & r \end{pmatrix} \begin{pmatrix} T_1 \\ T_2 \end{pmatrix} + \begin{pmatrix} 0 \\ m_g g \\ 0 \end{pmatrix} \tag{4}$$

For a free-flying aircraft, $m_x = m_z = m_g$. Our experimental apparatus is mounted on a stand and has different inertial masses in the horizontal and vertical directions m_x and m_z, respectively, and a different gravitational mass m_g. The inputs T_1 and T_2 are the longitudinal and perpendicular components of the thrust in body coordinates. Typically, T_1 is much larger than T_2. The pitch angle θ is measured with respect to the horizontal. Because our model can fly in both horizontal directions, it is convenient to have a symmetric reference for the pitch angle. We use the symbol Θ for the angle with the vertical, measured positive in the same direction as the pitch angle.

It was shown in Ref. 16 that, if we ignore the aerodynamic terms, the system (4) becomes flat, with flat outputs given by the coordinates of the center of oscillation:

$$x_f = x + (J/m_x r)\cos\theta, \qquad z_f = z - (J/m_z r)\sin\theta \tag{5}$$

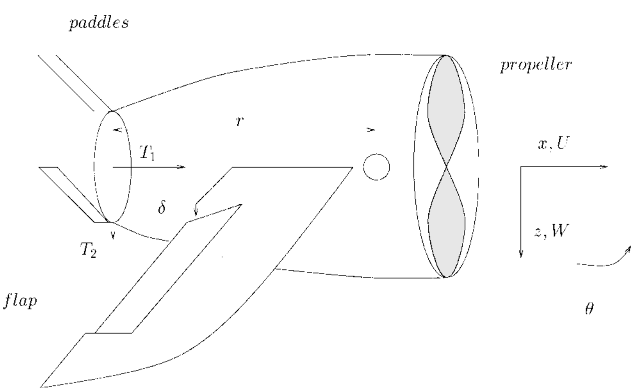

Fig. 2 Thrust-vectored aircraft with wing.

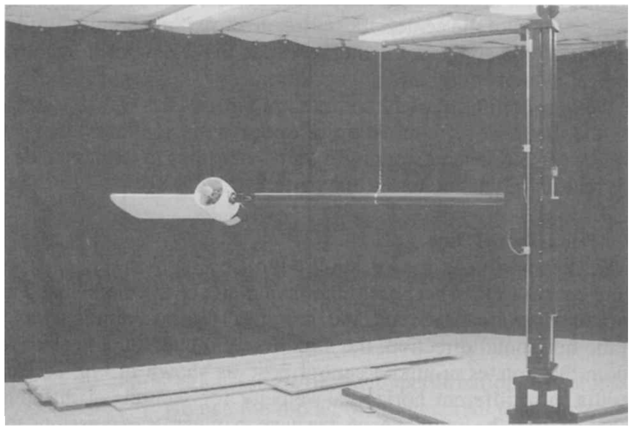

Fig. 3 Second-generation Caltech ducted fan with wing (photography courtesy of R. Bodenheimer).

As discussed in Sec. II, flatness means that all states and inputs of the system can be expressed as functions of the flat outputs and their derivatives. In particular, in this system,

$$\tan\theta = \frac{-m_z\ddot{z}_f + m_g g}{m_x\ddot{x}_f} \tag{6}$$

This equation gives us θ, and from θ and (x_f, z_f) we can find the other states. We can resolve the modulo π redundancy in the tangent function by requiring that the nose always be pointing forward.

For flat systems, trajectory planning becomes trivial: We can design a trajectory in the lower-dimensional output space and lift it to the full state and input space. For mode switching, we are interested in steering from an initial condition to a final condition. This gives prescribed values for the flat outputs and their derivatives at the initial and final time, which we then can link by an arbitrary curve in output space. Typically, one parameterizes the curves by basis functions, and then solves for the coefficients to match the initial and final conditions. See Refs. 17 and 18 for a more detailed treatment of trajectory planning for flat systems.

B. Aerodynamic Forces

Aerodynamic forces are most conveniently expressed in body coordinates. Hence, we rewrite Eqs. (4) in body coordinates as

$$\begin{pmatrix} m_U\dot{U} \\ m_W\dot{W} \\ J\dot{Q} \end{pmatrix} = \begin{pmatrix} T_1 \\ T_2 \\ rT_2 \end{pmatrix} + m_g g \begin{pmatrix} -\sin\theta \\ \cos\theta \\ 0 \end{pmatrix} + \begin{pmatrix} -m_W W Q \\ m_U U Q \\ 0 \end{pmatrix} + \frac{1}{2}\rho V^2 S \begin{bmatrix} C_x(\alpha, \delta_e) \\ C_y(\alpha, \delta_e) \\ \bar{c}C_\theta(\alpha, \delta_e) \end{bmatrix} \tag{7}$$

where $V^2 = U^2 + W^2$ is the square of the absolute velocity, ρ is the density of air, S is the wing surface, $\bar{c}$ is the mean aerodynamic chord, δ_e is the flap angle of the control surface, in our case an elevator, and $\alpha = \arctan(-W/U)$ is the angle of attack. The functions C_x, C_y, C_θ represent aerodynamic lift, drag, and moment, rotated from the wind frame to the body frame. The masses m_U and m_W now vary with pitch angle θ. If we omit the aerodynamic lift, drag, and moment in Eqs. (7), the model will still be flat, with the flat outputs $(\dot{x}_f, \dot{z}_f)$ as in Eqs. (4), but with body quantities substituted. Note that these outputs are not the velocity of the center of oscillation in body coordinates, but rather the spatial velocity expressed in body quantities.

It may seem from Eqs. (7) that we are dealing with a fully actuated system. However, the elevator is only effective in a narrow range around zero angle of attack, and for fast maneuvering we are interested in regimes with high angle of attack. We can use the elevator to trim and control the equilibrium in forward flight, but not to switch modes.

It may be that we are not interested in the x position, but only in the forward velocity, and also position in the spatial z coordinate, as in constant-altitude flight. Then, we can use the x velocity and the z position of the center of oscillation as our flat outputs. Similar considerations apply in the unlikely case that we want to regulate vertical velocity and horizontal position.

We propose to calculate nominal trajectories for the flat system (4) and use these as nominal trajectories for the nonflat system (7). We investigate several straightforward extensions to flatness to deal with the aerodynamic terms that perturb flatness.

C. Wind-Tunnel Data

We obtain expressions for the aerodynamic forces in Eqs. (7) from wind-tunnel tests. There are three main parts to the modeling. The horizontal boom, the shroud, and the wing. To allow unlimited travel in the horizontal direction, the aircraft is mounted on a horizontal boom that rotates around a central post, as shown in Fig. 3. This results in a different horizontal velocity for sections at different distance from the boom; hence, we have to integrate expressions for aerodynamic lift, drag, and moment over the radial distance to the center.

The boom is modeled as a cylinder, providing drag only and no lift and moment. The wing is a NACA 0015 airfoil,[19] which stalls at $\alpha = 15$ deg. This airfoil is symmetric, because we want to fly in both positive and negative directions. Wind-tunnel tests showed that the aerodynamic center is at the quarter-chord point for low angles of attack and for wind speeds $0 \leq v_x \leq 12$ m/s. The wing has an elevator hinged at the $\frac{3}{4}$-chord point, which can be rotated over $-60 \leq \delta_e \leq 60$ deg. For the shroud, we approximated the lift, drag, and moment by a fourth-order polynomial in wind speed, angle-of-attack paddle deflection, and elevator deflection. Including all cross terms and pruning terms with small coefficients, this results in some 50 terms.

Figure 4 shows the lift, drag, and moment as a function of airspeed and angle of attack, for $\delta_e = 0$, horizontal flight, zero paddle deflection, and zero thrust. Note the interesting sign reversal of the moment coefficient beyond the stall angle of attack. In this regime, the pitch moment dynamics are unstable. For small angles of attack, the center of pressure is aft of the center of mass by a distance of $d = 0.02$ m, resulting in stable pitch dynamics.

An interesting feature of the system is that level flight is not possible at all pitch angles. There is a range, roughly $-60 \leq \alpha \leq 60$ deg, beyond which the wing cannot generate enough lift to compensate for the weight (5 N). It appears crucial for mode switches to travel through this regime in a smooth manner. Appropriate feedforward is instrumental in achieving this transition. Even though the wing can generate enough lift for a range of angles of attack beyond stall, it is undesirable to fly at such high angle of attack for extended time because the increased drag results in much higher fuel consumption.

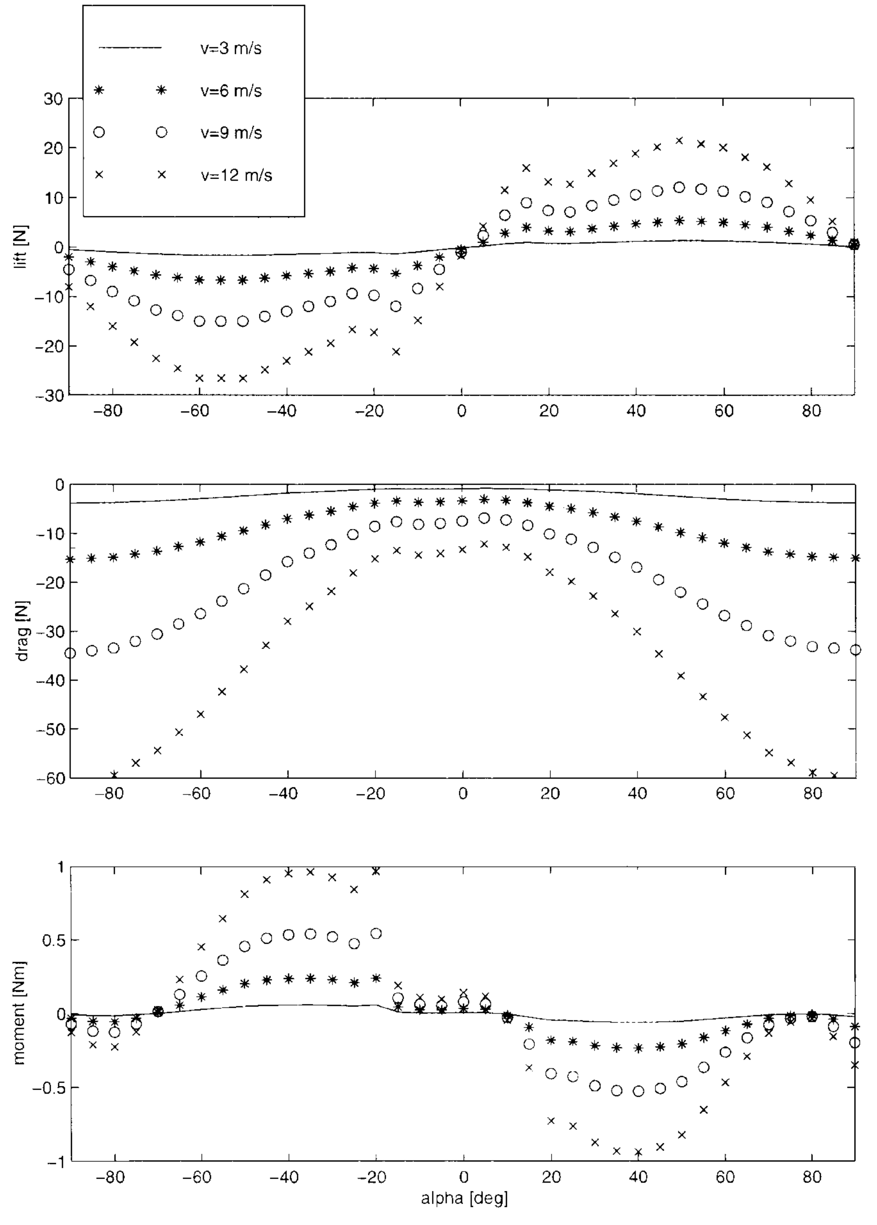

Fig. 4 Experimental lift, drag, and moment on thrust-vectored aircraft.

IV. Application of the Flat Model to the Full Aerodynamic Model

Because our experimental apparatus does not allow unlimited travel in the z direction, we only distinguish between hover and forward flight at constant altitude. This gives four possible transitions, the transition from forward flight to forward flight (at a different velocity) being most typical for normal flight, the transition from hover to forward flight being most interesting because of the regime in which the wing cannot carry the weight of the fan.

A. Pitch Dynamics and Pitch Trim Table

If we completely ignore the aerodynamics and only rely on the flat model (4) we generate a trajectory that does not steer to an equilibrium for the full aerodynamic system. It is shown in Ref. 20 with simulations that this approach leads to poor results, as could be expected. A first simple extension to the model (4) is to include the disturbance terms in the desired steady state. Even though the model (4) does not include aerodynamic forces, we need to account for these to establish steady-state forward flight. That is, we need to apply a certain force to balance drag, and we can use lift to balance gravity. If we restrict ourselves to horizontal forward flight, then from Eqs. (7) we can determine which forward-velocity and pitch-angle combinations establish a trim condition, i.e., lift equal to weight and zero moment. For certain forward velocities, there will be more than one pitch value that establishes trim. One corresponds to high angle of attack and therefore high drag; one corresponds to low angle of attack and low drag. It is the latter solution we are interested in for steady forward flight. From the forward velocity, we calculate the necessary pitch angle, which equals the angle of attack in horizontal flight, to generate the desired lift. We tabulate the pitch-speed trim conditions and interpolate from this table to find the pitch trim corresponding to a certain airspeed. The moment generated by the lift is balanced by the perpendicular thrust.

B. Flat Systems with Perturbations

In this section we investigate some aspects of the approximation of a nonflat system by a flat one. Suppose we have a nominal system that is flat and generate a nominal trajectory for it. We design a scheduled controller that stabilizes the system around the trajectory. Then, the error system, after transformation to error coordinates, becomes a linear system plus error terms:

$$\dot{x} = Ax + Bu + h(t, x) \tag{8}$$

Note that $h(t, x)$ contains perturbations to flatness and errors in the linearization, which might change along the trajectory. Therefore, $h(t, x)$ may still contain linear terms in x. Suppose we design a linear full state controller $u = Kx$, which gives us a quadratic Lyapunov function $V(x) = x^*Px$ such that

$$\dot{V}(x) = -x^*Qx + 2x^*Ph \tag{9}$$

for the linear system plus error, where $Q > 0$. Note that most linear controller design techniques provide a quadratic Lyapunov function. Now allow a correction in the input: $u = Kx + \delta u$; then, we get

$$\dot{V}(x) = -x^*Qx + 2x^*Ph + 2x^*PB\delta u \tag{10}$$

It follows that, if we pick δu to be the projection of h onto the range of B,

$$\delta_{\text{proj}} u = -B^{\dagger}h = -(B^*B)^{-1}B^*h \tag{11}$$

we will always decrease the perturbation in the derivative of V. We call this a compensation by projection. However, this error might actually be negative and help us decrease V. It is therefore advisable to check for the sign of this error before applying the correction (11). Moreover, we can do better: If x is not in the nullspace of B^*P, we can cancel the perturbation in Eq. (9) completely by setting δu equal to

$$\delta_2 u = -(x^*PB)^{\dagger}x^*Ph \tag{12}$$

Once again, we should only do this when the perturbation is positive. Obviously, even though the null space of B^*P is a thin set, the correction blows up for x almost aligned with the null space. We therefore need to incorporate some switching logic checking for the magnitude of x^*PB, resulting in a discontinuous correction based on decreasing the Lyapunov function V:

$$\delta_{\text{Lyap}} u = \begin{cases} \delta_2 u & \text{for} \quad x^*PB > \epsilon \quad \text{and} \quad x^*Ph > 0 \\ 0 & \text{otherwise} \end{cases} \tag{13}$$

where ϵ is some bound corresponding to the actuator limits. We call this a Lyapunov correction.

C. Simulations

We try the simple extensions to deal with perturbations to flatness on the model (7). We use the model (4) to generate the trajectory and simulate on the model (7), which includes aerodynamic terms. We simulate the aircraft with one wing only. This is because our experimental aircraft is mounted on a stand and has only one wing. For two wings, we would simply multiply the wingspan by two.

We denote the angle with the vertical as $\Theta = \theta - \pi/2$. Then, hover corresponds to $\theta = \pi/2 \Leftrightarrow \Theta = 0$. We plot the nominal (solid) and simulated (dashed) traces of the forward velocity v_x, the altitude $y = -z$, Θ, and the perpendicular [solid, T_2 in Eqs. (4)] and parallel thrust [dashed, T_1 in Eqs. (4)].

The maneuver we are trying to follow is a transition from hover to forward flight, at a speed of 6 m/s, in 6 s. The corresponding angle of attack that provides a lift equal to the weight (4.6 N) at this speed is $\alpha = 13$ deg or $\Theta = -1.34$ rad. Because in the transition regime the fan cannot lift its own weight, the transition will result in a drop in altitude in the nominal trajectory.

The controller used to stabilize around the trajectory is a gain-scheduled linear quadratic regulator (LQR) controller, scheduled in pitch. The controller has integrators on both v_x and z to ensure zero steady-state error, which is important in setpoint regulation.

First, we examine what happens if we use no model-based nominal trajectory, but try to follow a linear interpolation between hover and forward flight. Figure 5 shows that the lack of an appropriate feedforward term results in severe pitch oscillations and poor altitude response.

In Fig. 6, we generate a nominal trajectory that steers to the right trim condition, corresponding to (7). We see clear improvement: The error in altitude is significantly less. Notice the nonzero perpendicular force necessary to balance the moment on the wing due to nonzero moment coefficient C_m.

Finally, we compensate for the aerodynamic terms by a projection on the input space as described in Sec. IV.B, by Eqs. (11) and (12). It turns out that we get a worse response if we apply input correction (11). We checked that the perturbation in Eq. (9) is negative most of the time, and so canceling the term is detrimental. Applying the correction (12) does give a barely noticeable improvement in performance over that shown in Fig. 6. Again, we checked that the correction in the input is zero most of the time. See Ref. 20 for the corresponding plots.

We also examined a more aggressive maneuver from forward flight in the positive direction, $v_x = +6$ m/s to reverse flight, $v_x = -6$ m/s, in 12 s. We verified the same trends as with the hover-to-forward-flight transition: Adding the projective correction from Eq. (11) deteriorates performance, while adding the Lyapunov correction from Eq. (12) gives a small improvement in performance. See Ref. 20 for the plots.

V. Experiments

A. Description of Hardware and Software

Experiments are conducted on a model of a thrust-vectored aircraft built at Caltech. To allow unlimited travel in the horizontal direction, the aircraft is mounted on a horizontal boom that rotates around a central post, as shown in Fig. 3.

The aircraft is interfaced to an Intel 486 66-MHz personal computer. It uses a linear current amplifier to regulate the current to a 200-W electric motor, driving a propeller. Pulse width modulated (PWM) servos steer the thrust-vectoring paddles and the elevator.

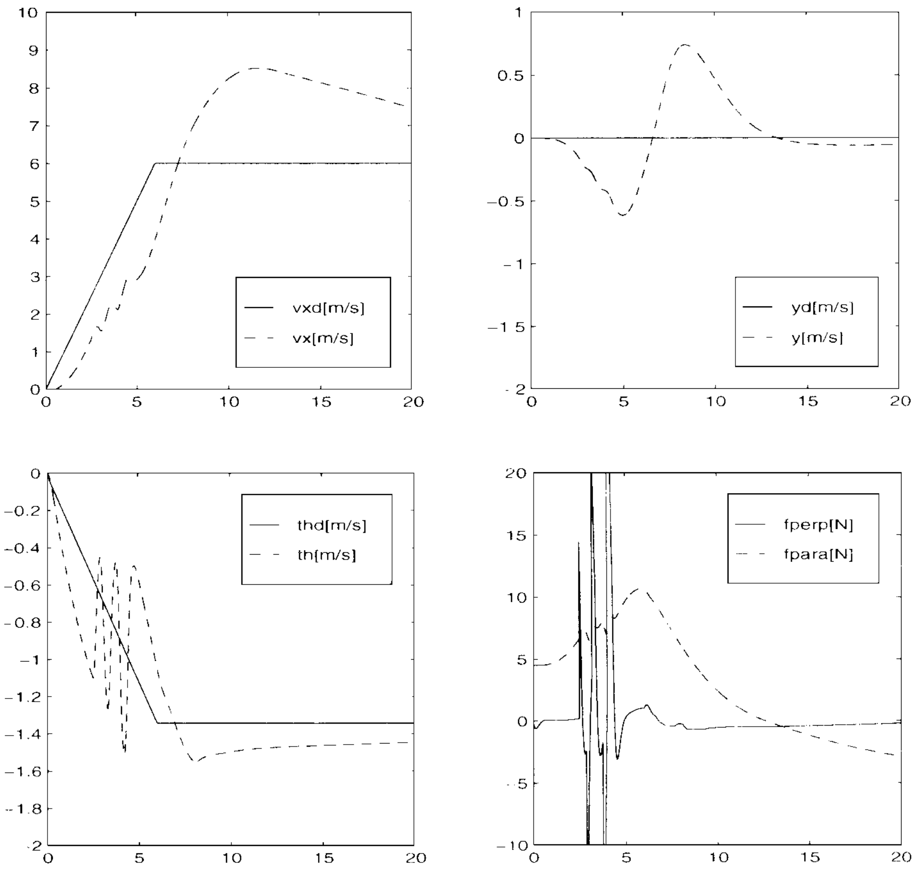

Fig. 5 Simulation of maneuver from hover to forward flight, one-DOF design.

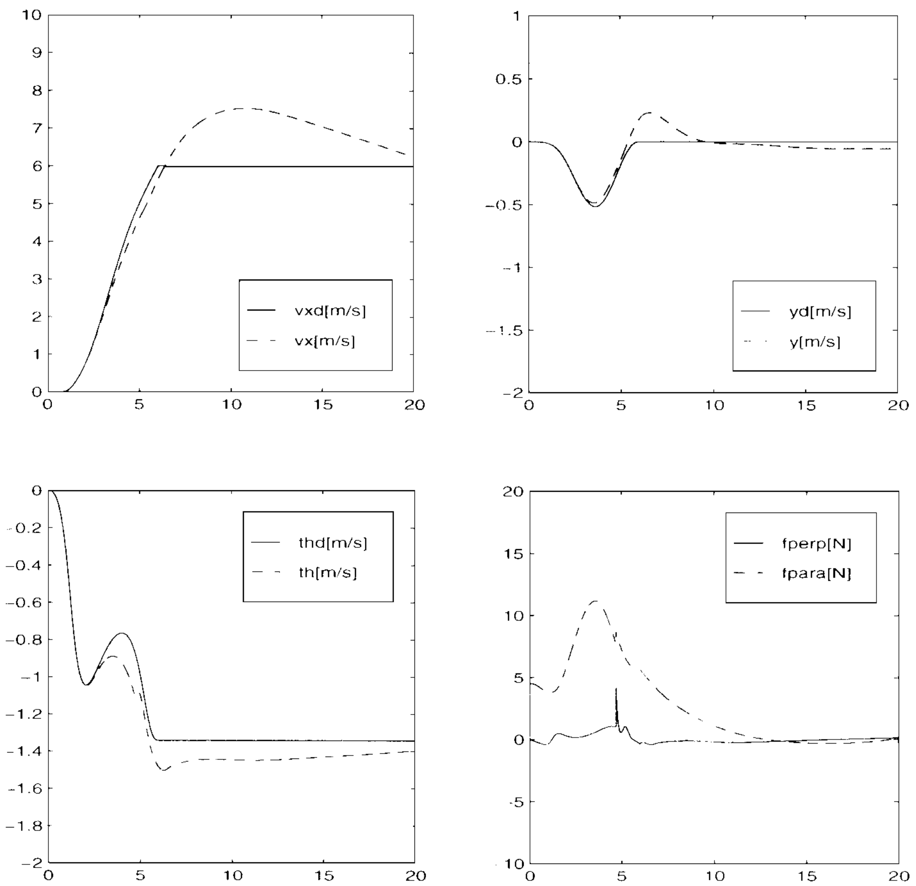

Fig. 6 Simulation of maneuver from hover to forward flight, two-DOF design steering to aerodynamic trim.

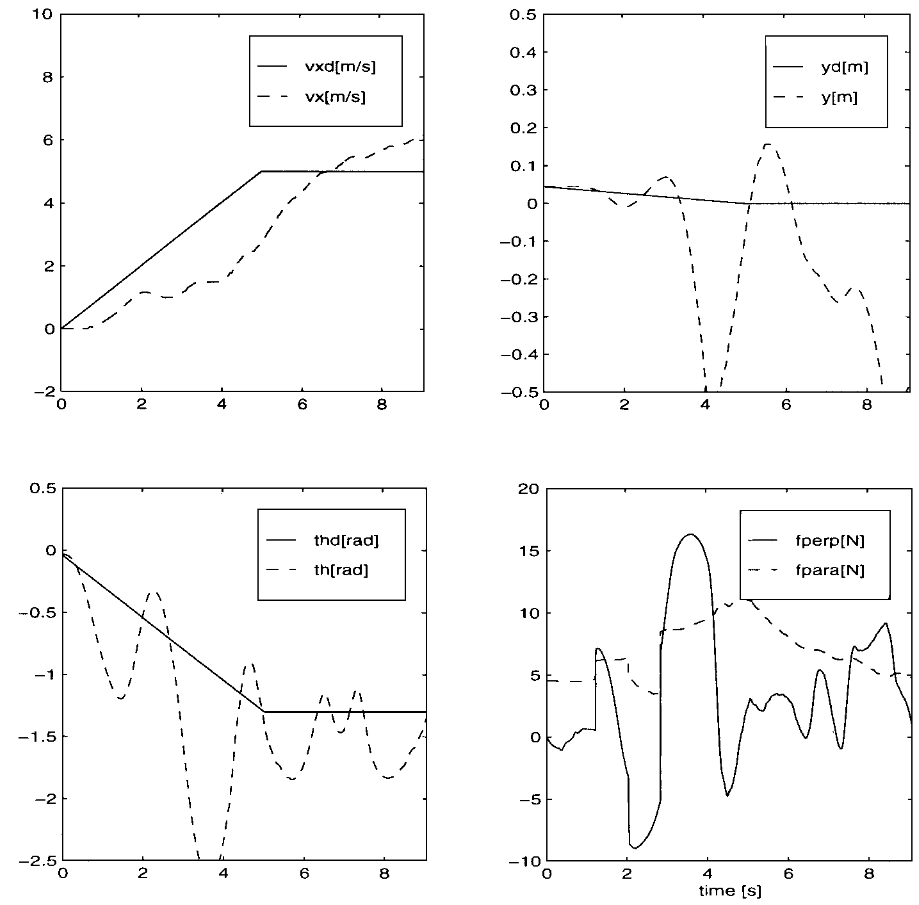

Fig. 7 Experimental results of hover to forward flight, one DOF.

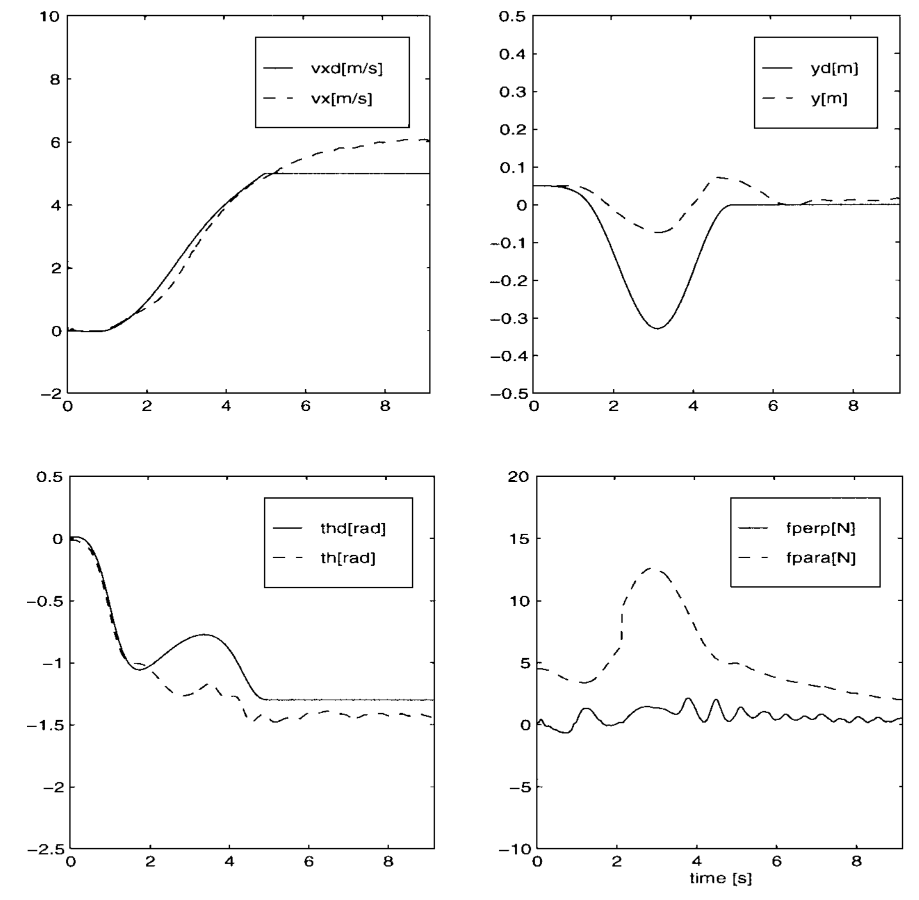

Fig. 8 Experimental results of hover to forward flight, two DOF.

The PWM signal is generated by a custom-built personal computer board. The airfoil is a NACA 0015. Horizontal, vertical, and pitch position are measured with encoders. Velocities are obtained by numerical differentiation and smoothing.

The gravitational mass of the fan is offset by a counterweight in the center of the central post to allow the motor to lift the weight of the fan and the boom in hover. To reduce the inertial mass in the vertical direction, this counterweight is attached through a pulley with gear ratio 1:5. This results in different gravitational masses ($m_g = 0.46$ kg) and inertial masses in the x and z directions ($m_x = 4.9$ kg and $m_z = 8.5$ kg), respectively. It was shown in Refs. 17 and 18 that using different masses does not affect flatness of the system (4). The numerical values of the other parameters in Eqs. (4) are $r = 0.12$ m, $J = 0.0323$ kg m^2, and $g = 9.8$ m/s^2.

The ducted fan is run with the real-time kernel Sparrow.[21] Sparrow takes care of reading sensor input, writing actuator output, data logging, and necessary controller computations.

Trajectory generation is done with the trajectory generation library tglib, developed by M. van Nieuwstadt at Caltech. This library is available through anonymous ftp from avalon.caltech.edu in the file /pub/vannieuw/software/trajgen.tar.gz. This file contains the libraries, examples, and documentation. The routines are in ANSI C and will compile under different platforms. In particular, the simulations presented in this paper used the library compiled on a UNIX platform, and the real-time experiments used the library compiled under MS-DOS.

B. Hover-to-Forward-Flight Transitions

Next, we report experimental results for the mode transition from hover to forward flight that was simulated in the preceding section. We use the same pitch-scheduled LQR controller as in the simulations. We measure x, z, and Θ directly and obtain their velocities by use of a digital filter.

Motivated by the simulation results, we only compare trajectories that steer to the right trim without compensating for aerodynamic terms. Figures 7 and 8 show experimental data for a transition from hover to forward flight at 5 m/s in 5 s, for one and two DOF, respectively. Even though the nominal trajectory calculated for the flat system and the linear interpolation for the one-DOF design look very similar, the improvement of two-DOF design is dramatic. The linear interpolation shows severe pitch and altitude oscillations. Note the significant error in altitude in Fig. 7, which is due to stiction in the stand.

To verify repeatability of the above experiment, we performed 10 runs of this experiment and collected the minimum and maximum. We verified that the repeatability is good, even for the one-DOF controller, but the two-DOF controller consistently outperforms the one-DOF controller. The plots can be found in Ref. 20.

VI. Conclusions

This paper investigates the use of differential flatness in the computation of nominal trajectories for the pitch dynamics of a thrust-vectored aircraft. The dynamics of the aircraft resulting from thrust vectoring are flat, whereas the aerodynamic forces act as perturbation terms. We study various ways to account for the perturbation terms so as to improve on the trajectories generated by the flat approximation. For experimental validation, we use the problem of mode switching, i.e., fast transitions between flight regimes with strongly different dynamics and actuator efficiencies.

Maneuvers involving transition to forward flight benefit from the use of a feedforward trajectory based on a flat approximation, provided that this feedforward trajectory steers to the right trim for the nonflat system. Appropriate feedforward terms allow a smooth transition between hover and forward flight without much change in altitude, over a regime in which no trim condition exists. Through a Lyapunov stability argument, we show that absorbing the error between the flat system and the flat approximation in the input may adversely affect tracking. This is because the error actually may make the Lyapunov function decrease faster.

It was shown in simulation and experiment that two-DOF design improves tracking for hover-to-forward-flight transitions. Much depends on the interplay between controller and feedforward, but, in general, we found that an appropriate feedforward term imposes lower bandwidth and gain requirements on the actuators. More research is needed to reach a conclusive answer about the benefits of two-DOF design in fast mode switching, but our preliminary results are promising.

Acknowledgments

Research supported in part by NASA, National Science Foundation Grant CMS-9502224, and Air Force Office of Scientific Research Grant F49620-95-1-0419. The authors would like to thank Mark Milam for his work on the ducted fan experiment. References 5, 20, and 21 are also available electronically from http://dubhe.cc.nps.navy.mil/~ gbradley/WorldVistas.html, http://www.cds.caltech.edu, and http://avalon.caltech.edu/~ sparrow, respectively.

References

[1]Etkin, B., *Dynamics of Atmospheric Flight*, Wiley, New York, 1985, pp. 271–293.

[2]McRuer, D. T., Ashkenas, I., and Graham, D., *Aircraft Dynamics and Automatic Control*, Princeton Univ. Press, Princeton, NJ, 1973, Chaps. 5 and 6.

[3]Herbst, W. B., "Dynamics of Air Combat," *Journal of Aircraft*, Vol. 29, No. 7, 1983, pp. 594–598.

[4]Herbst, W. B., "Future Fighter Technologies," *Journal of Aircraft*, Vol. 17, No. 8, 1980, pp. 561–566.

[5]McCall, G. H., and Corder, J. A. (eds.), *New World Vistas: Air and Space Power for the 21st Century*, Summary Volume, U.S. Air Force, Federal Information Exchange, Gaithersburg, MD, 1996, pp. 15–53.

[6]Martin, P., "Aircraft Control Using Flatness," *Computational Engineering in Systems Applications*, CESA, 1996, pp. 194–199.

[7]Van Nieuwstadt, M., and Murray, R. M., "Fast Mode Switching for a Thrust Vectored Aircraft," *Computational Engineering in Systems Applications*, CESA, 1996, pp. 86–91.

[8]Fliess, M., Lévine, J., Martin, P., and Rouchon, P., "Sur les Systèmes Non Linéaires Différentiellement Plats," *Comptes Rendus Hebdomadaires des Séances de l'Academie des Sciences, Série I*, Vol. 315, 1992, pp. 619–624.

[9]Fliess, M., Lévine, J., Martin, P., and Rouchon, P., "Linéarisation par Bouclage Dynamique et Transformations de Lie-Bäcklund," *Comptes Rendus Hebdomadaires des Séances de l'Academie des Sciences, Série I*, Vol. 317, 1993, pp. 981–986.

[10]Van Nieuwstadt, M., Rathinam, M., and Murray, R. M., "Differential Flatness and Absolute Equivalence," *Proceedings of the IEEE Control and Decision Conference*, Inst. of Electrical and Electronics Engineers, New York, 1994, pp. 326–333.

[11]Cartan, E., "Sur l'Équivalence Absolue de Certains Systèmes d'Équations Différentielles et sur Certaines Familles de Courbes," *Œuvres Complètes*, Vol. 2, Gauthier–Villars, Paris, 1953, pp. 1133–1168.

[12]Cartan, E., "Sur l'Intégration de Certains Systèmes Indéterminés d'Équations Différentielles," *Œuvres Complètes*, Vol. 2, Gauthier–Villars, Paris, 1953, pp. 1169–1174.

[13]Sluis, W. M., "Absolute Equivalence and Its Applications to Control Theory," Ph.D. Thesis, Dept. of Mathematics, Univ. of Waterloo, Waterloo, ON, Canada, 1992.

[14]Kwakernaak, H., and Sivan, R., *Linear Optimal Control Systems*, Wiley, New York, 1972, Chaps. 3–5.

[15]Bugajski, D. J., and Enns, D. F., "Nonlinear Control Law with Application to High Angle-of-Attack Flight," *Journal of Guidance, Control, and Dynamics*, Vol. 15, No. 3, 1992, pp. 761–767.

[16]Martin, P., Devasia, S., and Paden, B., "A Different Look at Output Tracking—Control of a VTOL Aircraft," *Automatica*, Vol. 32, No. 1, 1994, pp. 101–107.

[17]Van Nieuwstadt, M., and Murray, R. M., "Approximate Trajectory Generation for Differentially Flat Systems with Zero Dynamics," *Proceedings of the IEEE Control and Decision Conference*, Inst. of Electrical and Electronics Engineers, New York, 1995, pp. 4224–4230.

[18]Van Nieuwstadt, M., and Murray, R. M., "Real Time Trajectory Generation for Differentially Flat Systems," *International Federation of Automatic Control Symposium*, Vol. E, International Federation of Automatic Control, San Francisco, 1996, pp. 425–430.

[19]Abott, I. H., and Von Doenhoff, A. E., *Theory of Wing Sections Including a Summary of Airfoil Data*, Dover, New York, 1959.

[20]Van Nieuwstadt, M., "Trajectory Generation for Nonlinear Control Systems," Ph.D. Thesis, Dept. of Mechanical Engineering, California Inst. of Technology, Pasadena, CA, 1996.

[21]Murray, R. M., Wemhoff, E. L., and Kantner, M., "Sparrow 2.1 Reference Manual," California Inst. of Technology, Pasadena, CA, 1995.